

TEM Study of Rhodium Catalysts with Manganese Promoter

A. Merritt

Department of Physics, Purdue University, West Lafayette, Indiana, 47907

Y. Zhao and R.F. Klie

Department of Physics, University of Illinois at Chicago, Chicago, Illinois, 60607

The focus of this research is on studying the effects of a manganese promoter on rhodium particles for the purposes of ethanol catalysation from syngas. Through TEM imaging, the particle size has been studied both before and after reduction with and without a manganese promoter. For pure rhodium on silica, the average particle size before reduction was 3.1 ± 0.8 nm and 3.1 ± 0.8 nm after reduction. For rhodium with a manganese promoter on silica, the average particle size before reduction was 2.3 ± 0.5 nm and 2.4 ± 0.7 nm after reduction. These results point to a clear effect of manganese on the particle sizes of rhodium, but an insufficient effect on particle size to fully explain all effects of manganese promotion on rhodium catalysts. Further research will be focusing on using a JEOL-2010F to conduct electron energy loss spectroscopy (EELS) and Z-contrast imaging structural studies.

Introduction

In the modern world, doubt over a consistent petroleum supply has led to increased research on alternative fuel sources. One such alternative is ethanol, a simple hydrocarbon chain with the molecular formula C_2H_6OH . The most popular method for ethanol production is fermentation of carbohydrates, a process that has been in use for thousands of years to produce alcoholic beverages, but has only comparatively recently been adapted for industrial ethanol production. This process has several drawbacks, the most significant of which are the relative impurity of the end product and the low rate of production. Catalysation is an alternative ethanol production method; through the use of the Fischer-Tropsch (FT) process, syngas (a mixture of H_2 and CO) can be converted into ethanol, syngas itself being derived from various feedstocks such as coal gasification or organic gas (biogas). This process offers several advantages over traditional fermentation, significantly higher purity and production capacity, in direct contrast to fermentation¹.

Nonetheless, an effective catalyst is needed to ensure the usefulness of this process. Most importantly for industrial applications, a catalyst must have high selectivity, activity and longevity. As well, the usage of a promoter, which is a material that affects the characteristics of a catalyst without being a catalyst itself, can improve all of these characteristics. However, contemporary research on catalyst effectiveness and promoters is sparse, consisting mostly of empirical studies¹. Results from previous studies are that rhodium syngas catalysts with manganese promoters have increased selectivity for ethanol over methane as well as increased activity². A fundamental understanding of catalysation mechanics and catalyst-promoter interaction is important to further develop the field.

The focus of this research project is on rhodium catalysts with a manganese promoter. Empirical research shows that rhodium is an ineffective catalyst of syngas for ethanol production, but that manganese acts as a promoter, improving the selectivity and activity of the rhodium¹³. H. Trevino reports that the addition of Mn to Rh catalysts on zeolite NaY support increases the selectivity of oxygenates, namely ethanol and ethyl acetate, without an increase in activity during immersion in NaOH solution⁴. F. van der Berg et al report that RhMnMo exhibits greatly increased selectivity for ethanol as well as increased activity compared to pure Rh on a silica support⁵. Wilson et al report, in contrast, that the addition of Mn to Rh catalysts in a silica gel has no significant impact on selectivity but leads to a tenfold increase in activity⁶. More recent research by T. Feltes confirms the increase in both selectivity and activity of Mn promoted Rh catalysts for ethanol catalysation from syngas². The content of these studies all point to a need for a better fundamental understanding of the role of Mn in the promotion of Rh catalysts with respect to particle size.

In order to explore the interaction, transmission electron microscopy (TEM) will be used to study the effects of manganese loading on rhodium particle size and distribution on a silica (SiO_2) substrate. The usage of high-energy electrons to image the samples provides the capability to measure the sizes of rhodium particles down to approximately 1 nm in diameter. A study of rhodium particle size is expected to improve understanding of the impact of manganese promotion on rhodium particle size, from which conclusions can be extended to the impact of the particle size on syngas catalysation.

Method

Various methods exist to load rhodium onto a silica support, and then add the manganese promoter; a discussion of these techniques is beyond the scope of this report, but previous authors can offer insight into this process². An important step in the preparation process is the calcination and reduction of the sample. After the rhodium and manganese are loaded, the sample is calcined by heating in air to 350°C for four hours, and then reduced by heating to 300°C for 2 hours under an H₂ flow, in the end leaving a pure catalyst particle on the support; it is at this stage that the focus of this research lies: in studying the effect of a manganese promoter on the effect of the calcination-reduction process for rhodium. This process is essential for rendering the catalyst usable², and so is of great interest to the scientific and industrial communities.

The powdered samples are prepared by taking bulk silica and adding rhodium and manganese through the dry impregnation process, whereby just enough metal solution is used to fill the pore volume of the silica support². This bulk sample is then ground with mortar and pestle to a fine powder. A small part (<1 gram) of this powdered sample is then mixed with approximately 20 mL of DI water and sonicated for 20 minutes to reduce the average silica particle size. A holey copper grid is immersed in this solution twice, and allowed to dry in air after each immersion. The final product has enough sample deposits for the purposes of this study.

For the TEM work, a JEOL-3010 TEM was used. This instrument is capable of 2 Å resolution. For the purposes of this study, phase contrast imaging was used, whereby plane electron waves are distorted slightly by an incident material's structure, producing a phase difference between the diffracted electrons and the undiffracted ones and a change in intensity at the imaging point. The fact that the rhodium particles have a crystalline structure versus the amorphous silica support makes this technique effective, as the rhodium particles appear as dark spots on a gray background. In addition, the normal mas-thickness contrast imaging aided recognition of the heavier rhodium particles when the phase difference was insufficient.

For the study, the promoted rhodium unreduced sample was used for an in situ reduction study. The sample was heated in the vacuum of the microscope, approximately 10⁻⁷ torr, in order to drive off the oxide layer. After two hours, the sample was imaged and analyzed. The sample was allowed to cool to room temperature over two hours, and imaged again. This was done to compare reduction processes as a control.

A typical TEM image for this project is shown below (Fig. 1). Images are taken at ×300k magnification using

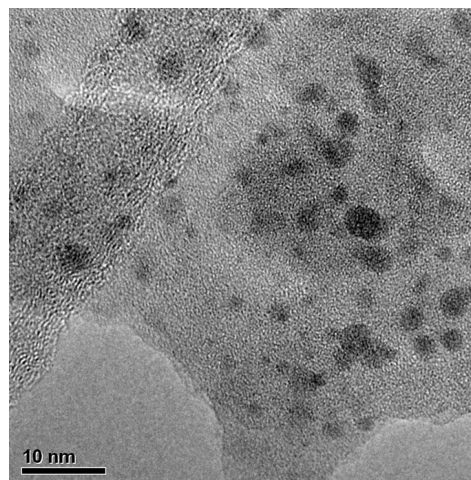


FIG. 1: TEM image of Rh particles on SiO₂ substrate. Rhodium particles are dark, the gray is the silica support, the bottom right is empty space.

a Gatan 1k × 1k CCD Camera on autoexposure, and interpreted using the Gatan Digitalmicrograph program. This program uses information stored in the image file of the setup to, amongst other features, convert pixel distances into actual distances, allowing the measuring of lengths in the image.

Data and Analysis

For each preparation method, the ten best images are selected out of all those taken and used to obtain an average particle size. Ten particles are used from each image for 100 particles in total per preparation method. For pure rhodium on silica, the average particle size was 3.1 ± 0.8 nm before reduction and 3.1 ± 0.8 nm after reduction. For rhodium with a manganese promoter on silica, the average particle size was 2.3 ± 0.5 nm before reduction and 2.4 ± 0.7 nm after reduction. For the in situ heated promoted catalysts, the average particle size was 2.6 ± 0.9 nm before reduction and 2.4 ± 0.7 nm after reduction. A histogram representative of the particle size distribution is shown in Figure 2. The particle size results are compared Table I.

Sample	Average Particle Size (nm)	Standard Deviation (nm)
RhO _x (unreduced)	3.1	0.8
Rh+Mn O _x (unreduced)	2.3	0.5
Rh+Mn	2.4	0.7
Rh+Mn (in situ heating)	2.6	0.9
Rh+Mn (after cooling)	2.4	0.6

TABLE I: Particle size results.

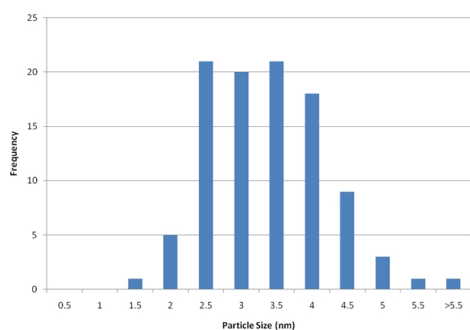


FIG. 2: Unreduced rhodium particle size distribution as a histogram.

Particle Measurement Errors

Errors in using the Digitalmicrograph program can be divided into two categories: orientation and line-laying errors. The former refers to taking the length measurement along different axes of a particle, due to the imperfectly spherical nature of a rhodium particle, and was found to be an average of 0.2 nm. The latter error refers to the imperfect boundaries of the particle in the image, resulting in imperfect starting and ending points for a length measurement; it averaged 0.2 nm after testing. The error due to taking a chord instead of a diameter is assumed to be contained in the line-laying error, and so is not counted separately. As well, the minimum pixel distance at x300k magnification is 0.11 nm, but this is subsumed in the line-laying error. The total read error then (per particle) is 0.4 nm, which for the purposes of the average reduces to 0.04 nm with 100 test particles as $\delta_a = \frac{\delta}{\sqrt{n}}$, which is far less than the standard deviation.

Discussion

The largest problems occur in imaging the catalyst specimens. As the rhodium particles are only a few nanometers in diameter, drift of portions of a nanometer in the time it takes to capture an image (on the order of a second) can seriously impede progress. Thus, improvements could be made to minimize drift and so improve the contrast and resolution of the images, and thus increase the accuracy of particle size measurements.

Secondary imaging concerns are hydrocarbon contamination during imaging and poor contrast; these have been mitigated through decreased exposure time and usage of DI water for the former and decreased aperture size and improved focusing for the latter.

The current specimen preparation method has proven satisfactory as far as deposit distribution is concerned. However, work is needed to reduce the thickness of sup-

port material, as the current amount of silica underneath or above the rhodium particles significantly impacts the level of contrast attainable using the TEM.

Chromatic aberration in the thick samples is caused by electron scattering in the amorphous silica induces incoherent phase shifts in the plane electron wave impinging on the specimen. The reduced coherence of the electron beam then influences the diffraction of the constituent electrons through the rhodium particles, resulting in some electrons being randomly scattered. This produces a pronounced blurring and graying effect in the images, and contributes significantly to read error.

Note that the minimum particle size that can be measured is approximately 1.5 nm, at which point imaging is almost entirely through mass-contrast imaging; however, particles smaller than this do seem to appear in the TEM images, but it is impossible to reliably measure their diameter, and so they are not counted. Switching to a higher magnification may improve the ability to count these particles, but this would be difficult due to stability issues. The impact of ignoring these particles is most likely small, however, due to the very limited number appearing in images.

Conclusion

For pure rhodium on silica, the average particle size was 3.1 ± 0.8 nm before reduction and 3.1 ± 0.8 nm after reduction. For rhodium with a manganese promoter on silica, the average particle size was 2.3 ± 0.5 nm before reduction and 2.4 ± 0.7 nm after reduction. This points to a clear effect of the manganese on particle size and distribution. However, the particle size difference does not fully explain all phenomena associated with promotion of rhodium catalysts with manganese. In situ reduction establishes a control for prior reduction, and the two processes produce comparable results.

Future work will be focused on analyzing the samples with a JEOL-2010F capable of EELS and Z-contrast imaging. EELS enables the analysis of electronic characteristics of the specimen, such as oxidation state densities. This combined with the better resolution available through Z-contrast imaging, a different imaging technique, will allow studies of the density of certain oxidation states (notably Rh_2O_3 and RhO_2) in the rhodium particles, both with and without the manganese promoter. Further studies should reveal any differences in the spatial density of these states, as well as any interfacial interactions between the rhodium particles and the silica support.

Acknowledgments

The authors would like to thank the National Science Foundation and the Department of Defense for funding the Research Experience for Undergraduates (REU) program at University of Illinois at Chicago under EEC-NSF Grant # 0755115. As well, the authors would like

to thank professors Takoudis and Jurisch of UIC as the REU organizers, Ke-Bin Low of the UIC Research Resource Center East for his training and help with the JEOL-3010 TEM, and the Research Resource Center at UIC for their TEM expertise.

-
- ¹ J. J. Spivey and A. Egbebi, Chem. Soc. Rev. **36**, 1514 (2007).
 - ² T. Feltes, Ph.D. thesis, University of Illinois at Chicago (2010).
 - ³ G. C. Bond, in *Heterogeneous Catalysis, Principles and Applications* (Oxford Science Publications, 1987).
 - ⁴ H. Trevino, Ph.D. thesis, Northwestern University (1997).
 - ⁵ F. van den Berg, J. Glezer, and W. Sachtler, J. of Catal. **93**, 340 (1985).
 - ⁶ T. Wilson, P. Kasai, and P. Ellgen, J. of Catal. **69**, 193 (1981).
 - ⁷ V. Subramani and S. K. Gangwal, Energy Fuels **22**, 814 (2008).